



Article

# Generation of Flag/DYKDDDDK Epitope Tag Knock-In Mice Using *i*-GONAD Enables Detection of Endogenous CaMKII $\alpha$ and $\beta$ Proteins

Kazushi Aoto <sup>1,\*</sup> , Shuji Takabayashi <sup>2</sup> , Hiroki Mutoh <sup>1</sup> and Hirotomo Saitsu <sup>1,\*</sup>

<sup>1</sup> Department of Biochemistry, Hamamatsu University School of Medicine, Hamamatsu 431-3192, Japan

<sup>2</sup> Laboratory Animal Facilities & Services, Preeminent Medical Photonics Education & Research Center, Hamamatsu University School of Medicine, Hamamatsu 431-3192, Japan

\* Correspondence: kaz@hama-med.ac.jp (K.A.); hsaitsu@hama-med.ac.jp (H.S.); Tel.: +81-53-435-2327 (K.A.); +81-53-435-2325 (H.S.)

**Abstract:** Specific antibodies are necessary for cellular and tissue expression, biochemical, and functional analyses of protein complexes. However, generating a specific antibody is often time-consuming and effort-intensive. The epitope tagging of an endogenous protein at an appropriate position can overcome this problem. Here, we investigated epitope tag position using AlphaFold2 protein structure prediction and developed Flag/DYKDDDDK tag knock-in CaMKII $\alpha$  and CaMKII $\beta$  mice by combining CRISPR-Cas9 genome editing with electroporation (*i*-GONAD). With *i*-GONAD, it is possible to insert a small fragment of up to 200 bp into the genome of the target gene, enabling efficient and convenient tagging of a small epitope. Experiments with commercially available anti-Flag antibodies could readily detect endogenous CaMKII $\alpha$  and  $\beta$  proteins by Western blotting, immunoprecipitation, and immunohistochemistry. Our data demonstrated that the generation of Flag/DYKDDDDK tag knock-in mice by *i*-GONAD is a useful and convenient choice, especially if specific antibodies are unavailable.

**Keywords:** flag epitope tag; *i*-GONAD; CRISPR-Cas9 genome editing; AlphaFold2; Western blot; immunohistochemistry



**Citation:** Aoto, K.; Takabayashi, S.; Mutoh, H.; Saitsu, H. Generation of Flag/DYKDDDDK Epitope Tag Knock-In Mice Using *i*-GONAD Enables Detection of Endogenous CaMKII $\alpha$  and  $\beta$  Proteins. *Int. J. Mol. Sci.* **2022**, *23*, 11915. <https://doi.org/10.3390/ijms231911915>

Academic Editor: Alvaro Galli

Received: 24 August 2022

Accepted: 4 October 2022

Published: 7 October 2022

**Publisher's Note:** MDPI stays neutral with regard to jurisdictional claims in published maps and institutional affiliations.



**Copyright:** © 2022 by the authors. Licensee MDPI, Basel, Switzerland. This article is an open access article distributed under the terms and conditions of the Creative Commons Attribution (CC BY) license (<https://creativecommons.org/licenses/by/4.0/>).

## 1. Introduction

Genome-editing techniques, such as zinc-finger nuclease (ZFN), transcriptional activator-like effector nuclease (TALEN), and clustered regularly interspaced short palindromic repeats-Cas9 (CRISPR-Cas9), have dramatically reduced the time and cost of generating knockout, knock-in, and conditional knockout mice [1–4]. Classically, mutant mice are created by gene-targeting embryonic stem (ES) cells and microinjection into fertilized eggs [3,4]. Recently, *in vitro* electroporation [5,6] and improved genome editing via the oviductal nucleic acid delivery (*i*-GONAD) method [7,8] have been developed in animals, including mice, rats, and hamsters, and show a high productivity of between 50–80% success rate [7–10]. These methods can insert long DNA fragments, depending on the size of the synthesized single-stranded oligodeoxynucleotides (ssODNs), by homology-directed repair (HDR) mechanisms of double-strand breaks. Ohtsuka et al. [8] synthesized 1 kb long ssODNs from a messenger RNA template and developed knock-in mice with a fluorescent protein, mCitrine, but with a lower success rate of 15%. For most researchers, it is convenient to use commercially available 130 and 200 base pairs (bp) ssODNs. Since the length of homology arms for HDR needs to be more than the total length of 75–85 bp [11,12], it is possible to design homology arms within 70 bp or 140 bp for *i*-GONAD of the epitope tag.

Various commercially available and popular epitope tags have been used for knock-in mouse analysis, including the Flag/DYKDDDDK tag (8 amino acids (AAs)) of synthetic epitope tag [13–15], HA tag (YPYDVPDYA, 9 AA) of AA residues 98–106 of human influenza hemagglutinin [16,17], Myc tag (EQKLISEEDL, 10 AA) of C-terminal (AA residues 410–419) of human c-myc protein [18], V5 tag (GKPIPNPLLGLDST, 14 AA or shorter version IPNPLLGLD, 9 AA) of AA residues 95–108 of RNA polymerase alpha subunit of simian virus 5 [4], and fluorescent tags (GFP, RFP, etc.) [4]. Flag tags are commonly used for immunoprecipitation (IP), Western blotting (WB), and immunohistochemistry (IHC) in knock-in mice [13–15]. In many cases, epitope tag knock-in mice have been created by pronuclear microinjection into fertilized eggs [4,13–16]. The position of an epitope tag is important for protein function.

Calcium/calmodulin-dependent protein kinase type II subunit alpha and beta (CaMKII $\alpha$  and  $\beta$ ) regulate neuronal plasticity and memory [19], and are related to human disease and autosomal dominant intellectual disorders [20,21]. The three-dimensional (3D) structure and functional domain of CaMKII $\alpha$ / $\beta$  have already been reported [22]. It has been reported that in vivo Flag and HA tagging into the N or C-terminus of CaMKII $\alpha$  and  $\beta$  by in utero electroporation enables the rapid determination of the localization of endogenous CaMKII $\alpha$  and  $\beta$  proteins in the mouse brain [23]. However, epitope tag knock-in mice with CaMKII $\alpha$ / $\beta$  have not yet been produced.

In this study, we investigated the knock-in position of the Flag/DYKDDDDK tag based on the 3D model of protein structure predicted by the AlphaFold2 program [24,25] and developed CaMKII $\alpha$  and CaMKII $\beta$  knock-in mice using *i*-GONAD. Flag-CaMKII $\alpha$  and  $\beta$  proteins were confirmed using biological and histological assays. Our data showed that the Flag/DYKDDDDK tag knock-in mouse technique had advantages over a specific antibody-based assay.

## 2. Results

### 2.1. Investigation of Flag/DYKDDDDK Epitope Tag Position by AlphaFold2 Protein Structure Database

In the generation of epitope knock-in mice, we first determined the epitope tag position for the target protein. The epitope tag is a small peptide with a size of 8 to 14 AA, which can disrupt the target protein function when placed near the functional domain or localization domain in some cases [26,27]. CaMKII $\alpha$  and  $\beta$  proteins have a kinase domain in the N-terminal, a regulatory segment, a linker region in the middle, and an association domain in the C-terminal [22] (Figure 1a). We investigated the 3D structure of Flag-CaMKII $\alpha$  and Flag-CaMKII $\beta$  modeled by ColabFold: AlphaFold2 using MMseqs2 software (<https://colab.research.google.com/github/sokrypton/ColabFold/blob/main/AlphaFold2.ipynb>) (accessed on 16 March 2022) [24,25]. N-terminal peptides are well situated on the protein surface, and Flag peptides are very likely to be accessed by the anti-DYKDDDDK antibody (Figure 1b,c). Thus, the Flag/DYKDDDDK epitope tag at the N-terminal of CaMKII $\alpha$  and  $\beta$  appears to be promising for the generation of the epitope tag knock-in mice.

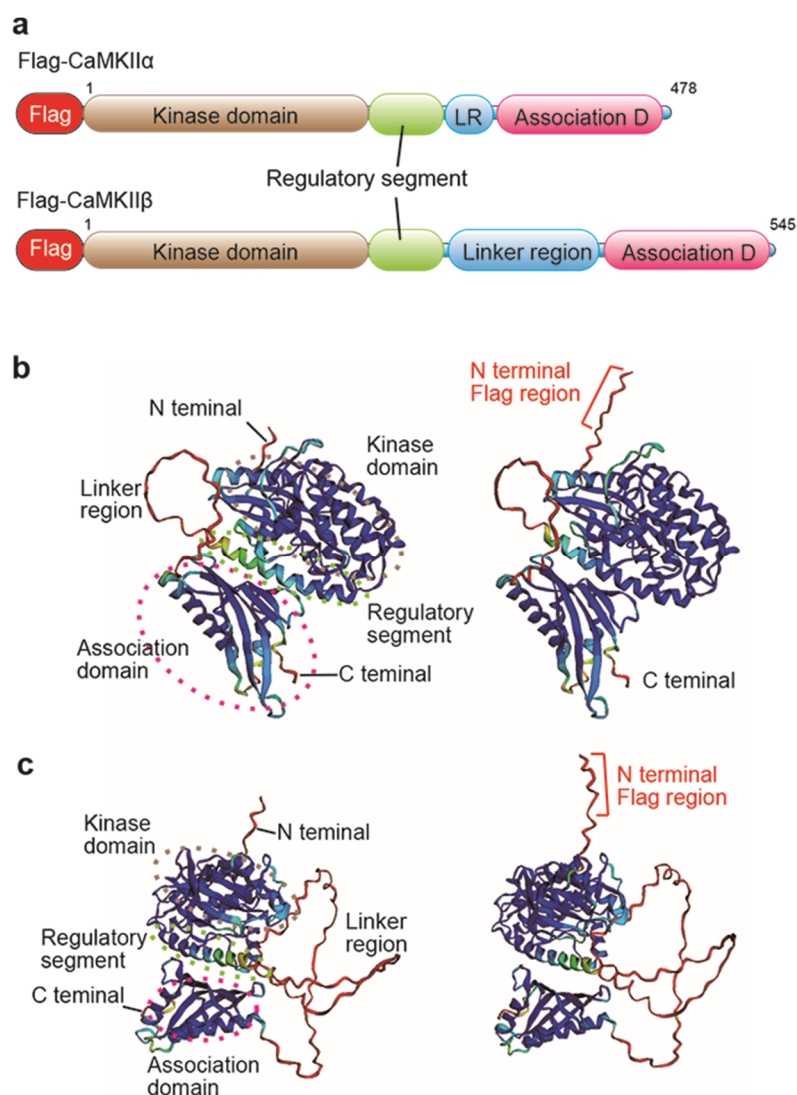


**Figure 1.** Flag-CaMKII $\alpha$  and  $\beta$  protein structures predicted by AlphaFold2. (a) Flag-tagged CaMKII $\alpha$  and CaMKII $\beta$  protein structures with a Flag tag (red), kinase domain (brown), regulatory segment (green), linker region (LR, blue), and association domain (pink). (b) 3D structure of CaMKII $\alpha$  (left) and Flag-CaMKII $\alpha$  (right) proteins by ColabFold. (c) The 3D structure of CaMKII $\beta$  (left) and Flag-CaMKII $\beta$  (right) proteins using ColabFold. The prediction quality as per residue confidence score, pLDDIT, is shown as colors of 3D structure, very high (blue, pLDDT > 90), confidence (light blue, 90 > pLDDT > 70), low (yellow, 70 > pLDDT > 50), and very low (red, pLDDT > 50).

## 2.2. Flag Knock-In Mouse Generation Using *i*-GONAD Method

To generate Flag/DYKDDDDK epitope tag knock-in mice, guide RNAs (gRNA) for CaMKII $\alpha$  and  $\beta$  were selected using CRISPR Targets track of the UCSC Genome Browser (<https://genome.ucsc.edu>) (accessed on 9 December 2017). Epitope tag knock-in mice were generated using *i*-GONAD. The HiFiCas9 protein, CRISPR RNA (crRNA), trans-activating crRNA (tracrRNA), and ssODNs were mixed, and the mixed solution was injected into the oviduct ampulla using a mouth glass capillary. After electroporation with an NEPA21 electroporator and electrode, the oviduct ampulla, ovary, and uterus were returned to the intra-abdominal cavity.

For CaMKII $\alpha$ <sup>N-Flag</sup> knock-in mice, six pups were obtained from four mothers: two wild-type pups, three knock-in pups, and one with deletion of several bases. For CaMKII $\beta$ <sup>N-Flag</sup> knock-in mice, a total of thirteen pups were born from four mothers: four wild-type pups, six knock-in pups, and three pups with deletions (Figure 2g). All pups were

genotyped by Sanger sequencing using specific primer sets around the knock-in region (Figure 2b,c,e,f and Figure S1). *CaMKIIα<sup>N-Flag</sup>* and *CaMKIIβ<sup>N-Flag</sup>* knock-in mice were crossed with outbred ICR mice for more than three generations to avoid potential off-target changes caused by CRISPR-Cas9 genome editing. Heterozygous (*N-Flag/+*) and homozygous (*N-Flag/N-Flag*) mice of *CaMKIIα<sup>N-Flag</sup>* and *CaMKIIβ<sup>N-Flag</sup>* did not show different body sizes and lengths, compared with wild-type mice. Moreover, both homozygous mice could mate with wild-type mice, indicating that the reproductive functions of the Flag-*CaMKIIα* and Flag-*CaMKIIβ* mice were normal. Thus, if a suitable tag position is selected using AlphaFold2, tag knock-in mice would reduce or minimize the dysfunction of the target gene.

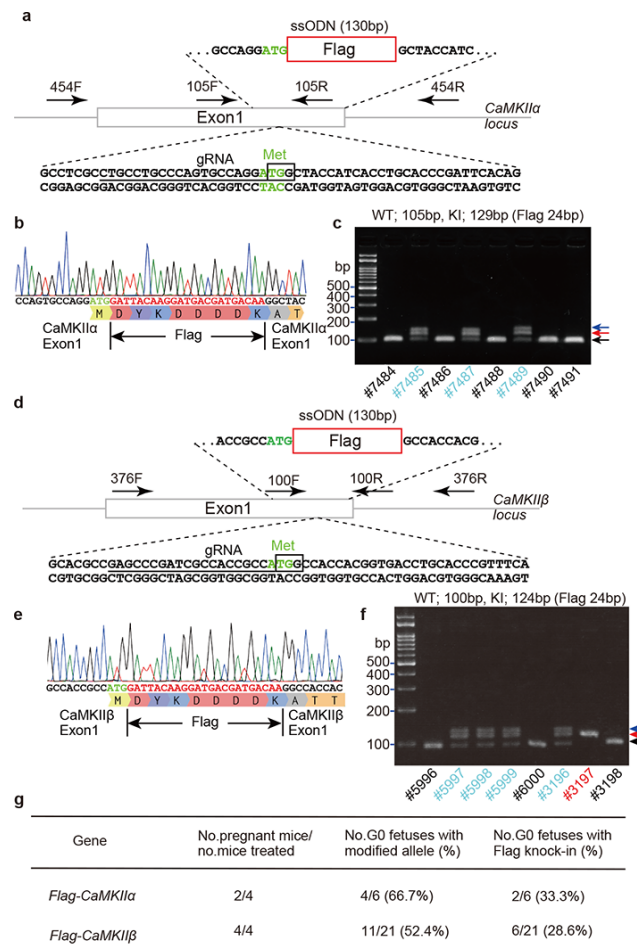


**Figure 2.** Generation of Flag knock-in mice for *CaMKIIα* and *CaMKIIβ*. (a) Sequence of exon 1 of mouse *CaMKIIα*, gRNA target site (black underline), and ssODN. The square box shows protospacer adjacent motif (PAM) sequence. The start codon encoding methionin (Met) is highlighted with green. (b) Confirmation of knock-in sequences. PCR products using genomic DNA as a template were cloned and sequenced. (c) Gel electrophoresis of PCR products amplified with primer sets of *CaMKIIα*-Ex1-105F/R in (a). Black and blue colored IDs indicate wild-type (WT) and knock-in (KI) pups, respectively. Black, red, and blue arrows show wild-type (105 bp), KI (129 bp) and heteroduplexed band of wild-type and KI DNA fragments, respectively. (d–f) Sequence of exon 1 of mouse *CaMKIIβ*, gRNA target site (black underline), and ssODN. Square box shows PAM sequence. The start codon encoding methionin (Met) is highlighted with green. (e) Confirmation of knock-in sequences. (f) Gel electrophoresis of PCR products amplified with primer sets of *CaMKIIβ*-Ex1-100F/R in (d). Black and blue-colored IDs indicate wild-type (WT) and knock-in (KI) pups, respectively. Black, red, and blue arrows show WT (100 bp), KI (124 bp) and heteroduplexed band, respectively. (g) A summary table of generating flag knock-in mice by *i*-GONAD.

### 2.3. Biochemical Assay Using *CaMKII $\alpha$ <sup>Fla</sup>* and *CaMKII $\beta$ <sup>Flag</sup>* Mice

To assess whether N-terminal Flag-tagged CaMKII $\alpha$  and  $\beta$  proteins were produced, we performed WB using commercially available anti-Flag/DYKDDDDK monoclonal antibody (clone 2H8) [28] in cortical, hippocampal, and cerebellar tissues of wild-type, *CaMKII $\alpha$ <sup>N-Flag</sup>* and *CaMKII $\beta$ <sup>N-Flag</sup>* mice. Flag-CaMKII $\alpha$  protein was strongly expressed in the cortex and hippocampus but weakly expressed in the cerebellum (Figure 3a). Flag-CaMKII $\beta$  was strongly expressed in the cortex, hippocampus, and cerebellum (Figure 3a). These results are similar to those of previous studies [29]. As expected, wild-type ICR mice did not show any specific bands. Next, as it is well known that CaMKII forms a dodecamer, in which  $\alpha$  and  $\beta$  subunits are predominant in the brain [22], we performed IP and WB using a cortical lysate of *CaMKII $\alpha$ <sup>N-Flag/N-Flag</sup>* homozygous knock-in mice to examine whether Flag-CaMKII $\alpha$  is associated with endogenous CaMKII $\beta$  proteins. Flag-CaMKII $\alpha$  bound to the endogenous CaMKII $\beta$  protein (Figure 3b). The Flag-CaMKII $\alpha$  protein showed a slightly shifted band, compared to the wild-type band, and its expression level was comparable to that of endogenous CaMKII $\alpha$  (Figure 3b, asterisk). The expression levels of CaMKII $\beta$  were also comparable between wild-type (WT) and *CaMKII $\alpha$ <sup>N-Flag/N-Flag</sup>* mice. These results indicate that Flag knock-in mice show a similar expression profile to that of endogenous CaMKII $\alpha$  and  $\beta$ , and Flag-CaMKII $\alpha$  works as a heterogeneous complex of probable dodecamers.

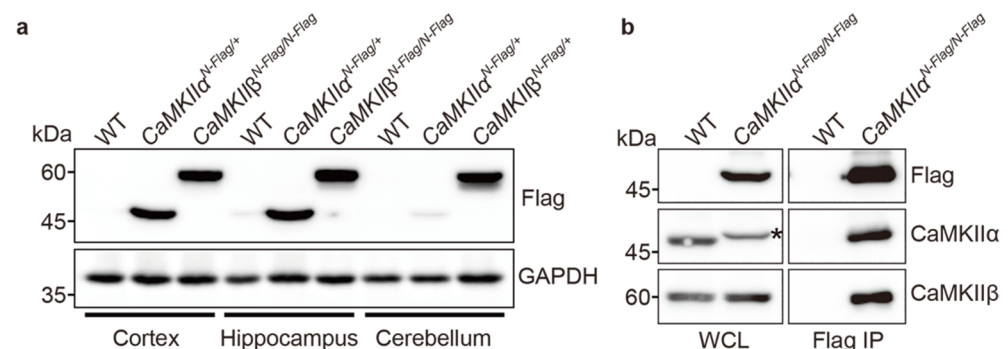


**Figure 3.** Expression of Flag-CaMKII $\alpha$  and  $\beta$  and association between Flag-CaMKII $\alpha$  and endogenous CaMKII $\beta$ . (a) Immunoblotting of cortical, hippocampal, and cerebellar samples in *CaMKII $\alpha$ <sup>N-Flag/+</sup>* heterozygous and *CaMKII $\beta$ <sup>N-Flag/N-Flag</sup>* homozygous knock-in mice using anti-Flag antibody. GAPDH was used as internal control. (b) Immunoblotting using anti-Flag, CaMKII $\alpha$ , and CaMKII $\beta$  specific antibodies, after immunoprecipitation of cortex sample in *CaMKII $\alpha$ <sup>N-Flag/+</sup>* mouse using flag antibody (Flag IP). WCL, whole cell lysate. Asterisk shows shifted band of Flag-CaMKII $\alpha$  protein, compared to that of endogenous CaMKII $\alpha$  protein.

### 2.4. Immunostaining Using *CaMKII $\alpha$ <sup>N-Flag</sup>* and *CaMKII $\beta$ <sup>N-Flag</sup>* Mice

Next, to examine the localization of Flag-CaMKII $\alpha$  and  $\beta$  proteins in the brain, immunostaining using anti-DYKDDDDK and anti-neuronal nuclei (NeuN) antibodies was performed on hippocampal CA1, cortex, and cerebellum of wild-type, *CaMKII $\alpha$ <sup>N-Flag/+</sup>* heterozygous, and *CaMKII $\beta$ <sup>N-Flag/+</sup>* heterozygous knock-in mice. Flag-positive cells were not found in wild-type ICR mice (Figure 4a,d,g). Flag-CaMKII $\alpha$  protein was strongly expressed in the neuronal cell bodies and axon/dendrites of the hippocampal CA1 and cortical layers, especially in the cell body and dendrites of cerebellar Purkinje cells, but not in the molecular layer and granular layer (Figure 4b,e,h). Flag-CaMKII $\beta$  protein was expressed in hippocampal and cortical neural cells and in all cell types of the cerebellum (Figure 4c,f,i). These results are similar to the published expression patterns of CaMKII $\alpha$  and  $\beta$  [30]. Moreover, Flag/DYKDDDDK staining in the hippocampal CA1 and dentate gyrus completely overlapped with the anti-CaMKII $\alpha$  antibody staining in *CaMKII $\alpha$ <sup>N-Flag/+</sup>* mice (Figure 4j–o). In this case, the anti-CaMKII $\alpha$  antibody detected endogenous CaMKII $\alpha$  and Flag-CaMKII $\alpha$  proteins. These results indicate that Flag knock-in for CaMKII $\alpha$  and

CaMKII $\beta$  enables the detection of FLAG-tagged proteins using commercially available epitope-specific antibodies.

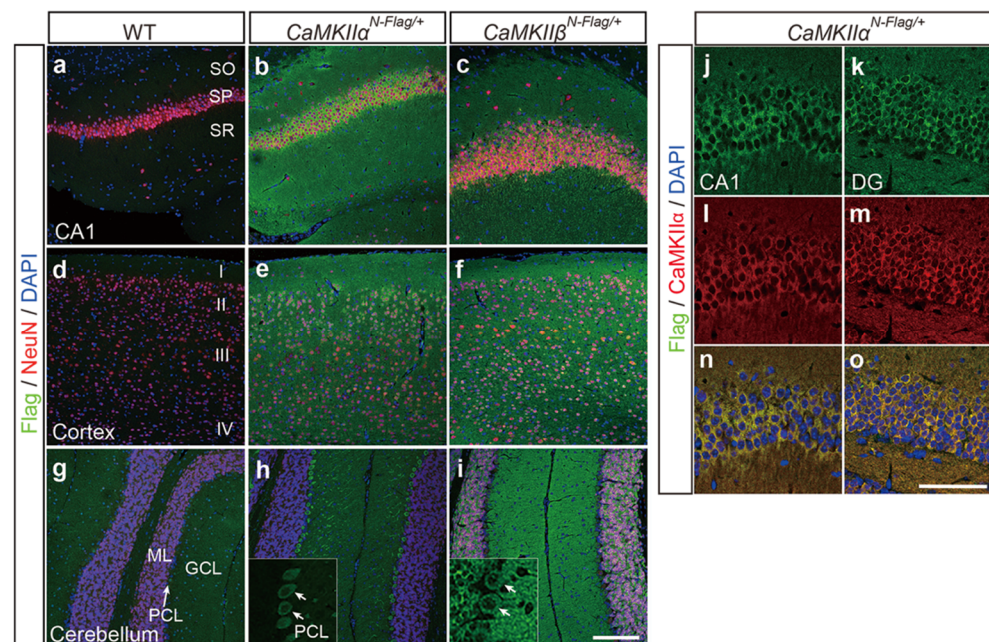


**Figure 4.** Detection of Flag-CaMKII $\alpha$  and Flag-CaMKII $\beta$  by immunohistochemistry. Immunostaining of hippocampal CA1 region (a–c), cortex (d–f), and cerebellum (g–i) of wild-type (WT, (a,d,g)), *CaMKII $\alpha$ <sup>N-Flag/+</sup>* (b,e,h), and *CaMKII $\beta$ <sup>N-Flag/+</sup>* (c,f,i) using anti-Flag (green) and neural marker anti-NeuN (red) antibodies. DAPI (blue) is nuclear marker. SO, stratum oriens, SP, stratum pyramidal, SR, stratum radiatum, SLM, stratum lacunosum-moleculare. Cortical layer I, II, III, and IV in D. ML, molecular layer, PCL, Purkinje cell layer, and GCL, granule cell layer. (j–o) Staining of anti-CaMKII $\alpha$  and anti-Flag/DYKDDDDK antibodies showed complete overlap in cytoplasmic region of hippocampal CA1 (j,l,n) and dentate gyrus (DG) (k,m,o) of *CaMKII $\alpha$ <sup>N-Flag/+</sup>* mice. Scale bar = 100  $\mu$ m in (a–i), 50  $\mu$ m in (j–o).

### 3. Discussion

Epitope tag knock-in mice are useful for protein expression and localization analysis. In expression vector or knock-in experiments, tag positions of target proteins are mainly in the N- or C-terminus of the target protein and in the middle, except for the functional domain and signal domain in very few cases [17,27]. This selection should be based on information on the 3D structure of the target protein. Our prediction method for determining the position of epitope tag knock-in using AlphaFold2 takes advantage of AlphaFold2-enabled highly accurate prediction of protein structures [24]. Our prediction results (Figure 1) were similar to the published 3D structural information for CaMKII $\alpha$  and  $\beta$  and its dodecamer [22]. The N- and C-terminal portions are shown in red in the 3D structure with a low confidence score (pLDDT), but both portions that are not alpha-helical bundles and beta-sheet domains should be considered as flexible protein structures that are amenable to tagging. AlphaFold2 also contributes to several biological processes, such as protein–protein complexes [31], prediction of the transcriptional activator domain [32], pathogenicity of missense variants [33,34], and phenotypic effects of single mutations [35]. Thus, our prediction for flag/DYKDDDDK epitope tag knock-in mouse is an application that uses structural modeling with AlphaFold2 and is able to escape the disruption of protein function by epitope tag.

The *i*-GONAD method is a powerful tool for rapidly producing CRISPR-Cas9 genome-edited mice and successfully producing N-terminal Flag/DYDDDDK tag knock-in mice against CaMKII $\alpha$  and  $\beta$  (Figure 2). In many epitope tag knock-in mice, the number of the epitope tag is increased as a tandem repeat of twice or triple for increasing epitope

recognition by antibody. In this study, we used a single Flag/DYDDDDK tag because the anti-DYKDDDDK monoclonal antibody, 2H8 clone, has high affinity for Flag/DYDDDDK tag protein sequence, but it can only be used for the detection of N-terminally tagged proteins [28]. One small tag may be preferable in terms of the potential risk of affecting target protein function by tagging and the higher success rate of knock-in because the success rate of gene knock-in would decrease depending on the increasing fragment size [36,37] and on the decreasing homology arm length [36,38].

The *i*-GONAD is a powerful method with high efficiency for knockout [6,8], or knock-in of short epitope tags and pathological single nucleotide variants (SNV) [6,8] and conditional knockout with loxP sequence [39] in mice (Figure 5, green round). The success rate of EGFP knock-in mice using synthesized ssODNs from a messenger RNA template was low at 15% [8] (Figure 5, orange round). However, to generate long insertional knock-in mice using more than 1 kb for many fluorescent proteins, reporter genes, Cre/Flippase recombinase, and replacement of human genes, we needed to develop a large fragment knock-in system (Figure 5, yellow round). Recently, an adeno-associated virus 1 or 6 (AAV1, AAV6)-mediated single-strand DNA delivery system for providing knock-in donors was shown to pass the zona pellucida surrounding the mouse oocyte and infect fertilized eggs [40,41]. Alternatively, the creation of a sufficient amount of long single-stranded strand DNAs would be useful, and double-strand DNA delivery by a gene targeting vector using the *i*-GONAD method would be much better if possible. Such technical developments would probably be able to create long-fragment knock-in mice using the *i*-GONAD method.

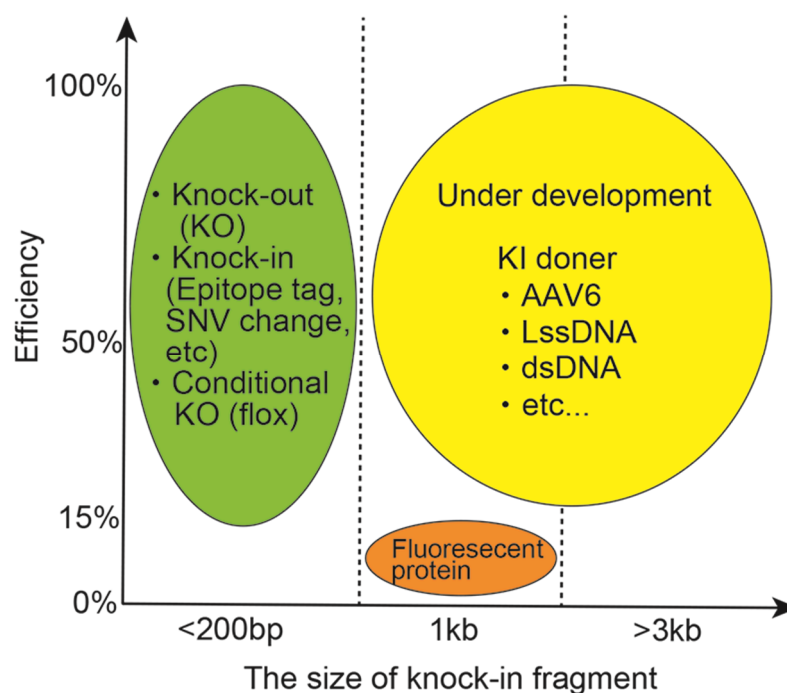


**Figure 5.** The *i*-GONAD efficiency for knock-out (KO), knock-in, and conditional KO. Schematic representation of genome editing efficiency and the size of knock-in fragment.

#### 4. Materials and Methods

##### 4.1. AlphaFold2 Analysis for Prediction of Flag Epitope Tag Position

The suitability of the FLAG epitope tag position for CaMKII $\alpha$  and CaMKII $\beta$  was estimated from the 3D structure of the proteins. The prediction of both protein structures was performed using ColabFold: AlphaFold2 with MMseqs2 (<https://colab.research.google.com/github/sokrypton/ColabFold/blob/main/AlphaFold2.ipynb>) (accessed on 16 March 2022) [24,25], CaMKII $\alpha$  (NP\_803126.1), and CaMKII $\beta$  protein sequence (NP\_001167524.1). The N-terminal Flag peptide sequence, DYKDDDDK, was added just after methionine protein of the translational initiation protein, similar to that of Flag/DYDDDDK tag knock-in mice.

#### 4.2. Flag Knock-In Mouse Generation Using *i*-GONAD Method

The *i*-GONAD method was performed, as previously described [7,8]. Experiments were performed in accordance with the guidelines of the Hamamatsu University School of Medicine Committee on Recombinant DNA Security (No. 3-25). All experiments were approved by the Hamamatsu University School of Medicine Animal Care and Use Committee (No. 2020019). ICR mice were purchased from Japan SLC, Inc. (Shizuoka, Japan). ICR mice were mated at evening 4–6 pm, and the next day, they were checked for plugs. In the evening time (4–6 pm) on the same day, plugged females were injected with CRISPR-Cas9 solution into the oviduct ampulla that was operated from the abdomen. The gRNA targets were selected as green in the UCSC genome browser (<https://genome.ucsc.edu>) (accessed on 9 December 2017). All CRISPR materials were purchased from Integrated DNA Technology, Inc. (IDT, Coralville, IA, USA) and Macrogen Inc. (Seoul, Korea) as the following name and sequence of gRNA and ssODN. CaMK2A-Ex1-gRNA: CTGCCTGCCCCAGTGCCAGGA. CaMK2B-Ex1-gRNA: GAGCCCCGATCGCCACCGCCA. Flag-CaMKII $\alpha$ -ssODN: CCCAGCCCTAGTTCCCAGCCTAAAGCCTCGCCTGCCTGCCCAGTGCCAGGATGGATTACAAGGATGACGATGACAAGGCTACCATCACCTGCACCCGATT CACAGAAGAGTACCAGCTCTTTGAGGA. Flag-CaMKII $\beta$ -ssODN: GCCGCCGCCGAGCGCAGCCGAGCGCACGCCGAGCCGATCGCCACCGCCATGGATTACAAGGAT GACGATGACAAGGCCACCACGGTGACCTGCACCCGTTTCACCGACGAGTACCAGC TATACGAGGA.

CRISPR-Cas9 solution contained as 30  $\mu$ M crRNA, 30  $\mu$ M tracrRNA, 1  $\mu$ / $\mu$ L HiFiCas9 protein, 1  $\mu$ / $\mu$ L ssODN, and 0.02% Fast Green in Opti-MEM (ThermoFisher, 31985062, Waltham, USA) and was filled into a glass capillary and injected into the oviduct ampulla in a total 1  $\mu$ L volume. After injection, the oviduct ampulla was covered with phosphate-buffered saline (PBS)-soaked KimWipes (Kimberly Clark Corp, Irving, USA) and was electroporated using an electrode under the following conditions (Porlin pulse: Voltage 50 V, pulse length 5 ms, pulse interval 50 ms, No. pulses 3, decay 10%, polarity +/–, transfer pulse: Voltage 10 V, pulse length 50 ms, pulse interval 50 ms, and no. pulses 3, Decay 40%, Polarity +/–) using a NEPA21 electroporator and tweezers without variable gap electrodes for Oviduct, CUY652P2.5X4 (NEPA GENE Co., Ltd. Ichikawa city, Japan).

#### 4.3. Genotyping of Flag-CaMKII $\alpha$ and Flag-CaMKII $\beta$

Genotyping PCR primers around the translational starting site of exon1 in the CaMKII $\alpha$  and CaMKII $\beta$  genes were selected based on the following names and sequences. PCR conditions was performed as 94 °C for 2 min, 30 cycles (98 °C for 10 s, 55 °C for 30 s, 68 °C for 30 s), 68 °C for 5 min. The wild-type band was 105 bp. The flag knock-in band was 129 bp using the following primer set. CaMK2A-Ex1-105F: TCAGCATCCCAGCCCTAGTTCCCAG. CaMK2A-Ex1-105R: CATGCTGCACACCTCCCTCTGCATG. CaMK2B-Ex1-100F: AGCCCGATCGCCACCGCCAT. CaMK2B-Ex1-100R: CGCGCCGAGGCTCTTACTTGC. CaMK2A-454F: CAGGCAGGTGTTGGGGAGGCAGTTA. CaMK2A-454R: CATGCTGCACACCTCCTCTGCATG. CaMK2B-376F: GCGGGACAGAGCGAGCAGATCTC. CaMK2B-376R: CTTGGGCCCGCAGCTGGAAGGAG.

#### 4.4. Immunoblotting and Immunoprecipitation

Brain tissues of CaMKII $\alpha$ <sup>Flag/+</sup> and CaMKII $\beta$ <sup>Flag/+</sup> mice at 8–12 weeks were collected, snap frozen in liquid nitrogen, and then stored at –80 °C until finishing genotyping and starting WB. Samples were lysed with 500  $\mu$ L RIPA buffer (150 mM NaCl, 50 mM Tris-HCl pH 7.4, 1 mM EDTA pH 8.0, 1% NP-40, 0.5% sodium deoxycholate, 0.1% SDS) supplemented with cOmplete Mini, EDTA-free Protease Inhibitor Cocktail Tablets (Roche, 11836170001, Basel, Switzerland through 10 passages with a 21G needle and syringe. After rotating on shaker for 30 min at 4 °C and centrifugation at 9100 $\times$  g for 10 min at 4 °C, supernatant samples were mixed with 2 $\times$  SDS sample buffer (0.125 M Tris-HCl pH 6.8, 4% SDS, 20% glycerol, 0.01% BPB, 100  $\mu$ L/mL 2-mercaptoethanol). For immunoprecipitation, the lysis solution was incubated with mouse monoclonal anti-DYKDDDK (clone 2H8)



(1/200 dilution, TransGenic Inc., Fukuoka, Japan), and Dynabeads ProteinG (VERITAS, DB10004, Tokyo, Japan). Boiled samples were separated by SDS-PAGE and transferred to a PVDF membrane (Clear Trans PVDF membrane, Hydrophobic, 0.45  $\mu$ m, 034-25663, FUJIFILM) with EzFastBlot (2332590, ATTO, Tokyo, Japan) using a semi-dry blotter (WSE-4115 PoweredBlot Ace, ATTO Corporation, Japan). After the transfer, the membranes were fixed with 4% paraformaldehyde (PFA, P6148-500G, Sigma-Aldrich, St. Louis, USA)/PBS for 30 min to increase the band signal. The membranes were blocked with 3% milk (Skim Milk Powder, 198-10605, FUJIFILM Wako Pure Chemical Corp., Osaka, Japan)/TBST (TBS + 0.1% Tween-20), and then incubated with the following primary antibodies: mouse monoclonal anti-CaMKII $\alpha$  (1/1000 dilution, 6G9 clone, #50049, Cell Signaling, Danvers, USA), rabbit anti-CaMKII $\beta$  (1/2000 dilution, GTX133072, Gene Tex, Irvine, CA, USA), mouse monoclonal anti-DYKDDDK (clone 2H8, 1/1000 dilution, TransGenic Inc., Japan), and mouse anti-GAPDH (1/50,000 dilution, 60004-1-Ig, Proteintech, Rosemont, USA) antibodies at 4 °C for overnight. The next day, after washing three times with TBST for 10 min, the PVDF membrane was incubated with the following secondary antibodies: goat anti-mouse and anti-rabbit antibodies conjugated with horseradish peroxidase (1/5000 dilution, Jackson ImmunoResearch, West Grove, PA, USA) for 1 h. After washing three times with TBST for 10 min, blotted membranes were detected using the Clarity Western ECL Substrate (#170-5060, Bio-Rad Laboratories, Inc., Hercules, FL, USA) for 5 min and FUSION-FX7. The EDGE Chemiluminescence Imaging System (M&S Instruments, Inc., Osaka, Japan).

#### 4.5. Immunohistochemistry

We analyzed two or more independent mice for each genotype. After transcardial perfusion with PBS and 4% PFA/PBS, the brains of FLAG tag knock-in mice at 8–12 weeks were dissected and fixed in 4% PFA/PBS solution overnight at 4 °C. After washing with cold PBS, the samples were dehydrated using an ethanol/xylene series and embedded in paraffin. Sectional samples were cut at 5  $\mu$ m thickness using a microtome (ThermoFisher HM430, USA) and placed on glass slides (MTSUNAMI, Platinum Pro, PRO-04, Osaka, Japan). After deparaffinization with xylene and 100% ethanol, and washing with 70% ethanol and running water for each 5 min, antigen retrieval was performed on sections with 10 mM sodium citrate solution with microwave for 10 min. A Super PAP pen Liquid Blocker (Daido Sangyo) was used to draw a hydrophobic circle around the brain tissue on a slide. After blocking with 3% BSA (albumin, from bovine serum, protease free, 018-15154, WAKO, Japan)/PBT (PBS plus 0.1% Tween-20 (sc-29113, Santa Cruz Biotechnology, Dallas, TX, USA) on the glass slides for 1 h at RT, sectional slides were incubated overnight at 4 °C with either of the following primary antibodies: mouse monoclonal anti-DYKDDDK (clone 2H8, 1/200, TransGenic Inc., Fukuoka, Japan) or rabbit anti-NeuN (1/500, ab177487; Abcam, Cambridge, UK). After washing three times with PBS, tissue slides were incubated for 1 h at RT with Alexa Fluor 488 or 546 donkey anti-mouse IgG and anti-rabbit IgG (1/200–1/400 dilution, A10036, Thermo Fisher Scientific, Waltham, MA, USA) as the secondary antibodies. After washing three times with PBS, the tissues were stained with the nuclear marker DAPI (1/1000 dilution, DOJINDO, NX034, Masushiro, Japan) and mounted with aqueous mounting media (Diagnostic BioSystems, Fluoromount/Plus, K048, Pleasanton, CA, USA). The mounted slides were imaged using a 20 $\times$  objective lens on a Leica TSC SP8 confocal microscope (Leica Microsystems, Wetzlar, Germany).

**Supplementary Materials:** The following supporting information can be downloaded at: <https://www.mdpi.com/article/10.3390/ijms231911915/s1>, Figure S1: The Sanger sequence including ssODN of knock-in region of CaMKII $\alpha$ N-Flag/N-Flag homozygous (a) and CaMKII $\beta$ N-Flag/+ heterozygous (b) mouse using 454F/454R primers for CaMKII $\alpha$  and 376F/R primers for CaMKII $\beta$ . Red square shows ssODN. Green square shows transcriptional starting site (TSS, ATG codon). Blue square shows Flag sequence. Pink bar shows exon1 region of mouse CaMKII $\alpha$  and CaMKII $\beta$  gene. Yellow arrow shows C insertion.

**Author Contributions:** K.A. performed experiments and wrote the original draft. S.T. created the knock-in mice. H.M. helped genotype the knock-in mice. H.S. provided the overall supervision, writing, and editing. All authors have read and agreed to the published version of the manuscript.

**Funding:** This work was supported by grants from Grants-in-Aid for Scientific Research (B) (20H03641) and (C) (20K07243, 21K05890, and 20K07423).

**Institutional Review Board Statement:** This study was conducted according to the guidelines of the Institutional Animal Care and Use Committee (IACUC) of the Hamamatsu University School of Medicine.

**Informed Consent Statement:** Not applicable.

**Data Availability Statement:** All data are available within the article and Supplementary Information. The materials of this study are available from the corresponding author upon request.

**Acknowledgments:** The authors thank Masumi Tsujimura and Kaori Shibazaki for their invaluable technical assistance.

**Conflicts of Interest:** The authors declare no conflict of interest.

## References

1. Li, H.; Haurigot, V.; Doyon, Y.; Li, T.; Wong, S.Y.; Bhagwat, A.S.; Malani, N.; Anguela, X.M.; Sharma, R.; Ivanciu, L.; et al. In vivo genome editing restores haemostasis in a mouse model of haemophilia. *Nature* **2011**, *475*, 217–221. [[CrossRef](#)] [[PubMed](#)]
2. Wang, H.; Hu, Y.C.; Markoulaki, S.; Welstead, G.G.; Cheng, A.W.; Shivalila, C.S.; Pyntikova, T.; Dadon, D.B.; Voytas, D.F.; Bogdanove, A.J.; et al. TALEN-mediated editing of the mouse Y chromosome. *Nat. Biotechnol.* **2013**, *31*, 530–532. [[CrossRef](#)]
3. Wang, H.; Yang, H.; Shivalila, C.S.; Dawlaty, M.M.; Cheng, A.W.; Zhang, F.; Jaenisch, R. One-step generation of mice carrying mutations in multiple genes by CRISPR/Cas-mediated genome engineering. *Cell* **2013**, *153*, 910–918. [[CrossRef](#)]
4. Yang, H.; Wang, H.; Shivalila, C.S.; Cheng, A.W.; Shi, L.; Jaenisch, R. One-step generation of mice carrying reporter and conditional alleles by CRISPR/Cas-mediated genome engineering. *Cell* **2013**, *154*, 1370–1379. [[CrossRef](#)]
5. Hashimoto, M.; Takemoto, T. Electroporation enables the efficient mRNA delivery into the mouse zygotes and facilitates CRISPR/Cas9-based genome editing. *Sci. Rep.* **2015**, *5*, 11315. [[CrossRef](#)] [[PubMed](#)]
6. Aoto, K.; Kato, M.; Akita, T.; Nakashima, M.; Mutoh, H.; Akasaka, N.; Tohyama, J.; Nomura, Y.; Hoshino, K.; Ago, Y.; et al. ATP6V0A1 encoding the  $\alpha$ 1-subunit of the V0 domain of vacuolar H(+)-ATPases is essential for brain development in humans and mice. *Nat. Commun.* **2021**, *12*, 2107. [[CrossRef](#)]
7. Gurumurthy, C.B.; Sato, M.; Nakamura, A.; Inui, M.; Kawano, N.; Islam, M.A.; Ogiwara, S.; Takabayashi, S.; Matsuyama, M.; Nakagawa, S.; et al. Creation of CRISPR-based germline-genome-engineered mice without ex vivo handling of zygotes by i-GONAD. *Nat. Protoc.* **2019**, *14*, 2452–2482. [[CrossRef](#)]
8. Ohtsuka, M.; Sato, M.; Miura, H.; Takabayashi, S.; Matsuyama, M.; Koyano, T.; Arifin, N.; Nakamura, S.; Wada, K.; Gurumurthy, C.B. i-GONAD: A robust method for in situ germline genome engineering using CRISPR nucleases. *Genome Biol.* **2018**, *19*, 25. [[CrossRef](#)]
9. Takabayashi, S.; Aoshima, T.; Kabashima, K.; Aoto, K.; Ohtsuka, M.; Sato, M. i-GONAD (improved genome-editing via oviductal nucleic acids delivery), a convenient in vivo tool to produce genome-edited rats. *Sci. Rep.* **2018**, *8*, 12059. [[CrossRef](#)]
10. Hirose, M.; Honda, A.; Fulka, H.; Tamura-Nakano, M.; Matoba, S.; Tomishima, T.; Mochida, K.; Hasegawa, A.; Nagashima, K.; Inoue, K.; et al. Acrosin is essential for sperm penetration through the zona pellucida in hamsters. *Proc. Natl. Acad. Sci. USA* **2020**, *117*, 2513–2518. [[CrossRef](#)]
11. Zhang, J.P.; Li, X.L.; Li, G.H.; Chen, W.; Arakaki, C.; Botimer, G.D.; Baylink, D.; Zhang, L.; Wen, W.; Fu, Y.W.; et al. Efficient precise knockin with a double cut HDR donor after CRISPR/Cas9-mediated double-stranded DNA cleavage. *Genome Biol.* **2017**, *18*, 35. [[CrossRef](#)] [[PubMed](#)]
12. Okamoto, S.; Amaishi, Y.; Maki, I.; Enoki, T.; Mineno, J. Highly efficient genome editing for single-base substitutions using optimized ssODNs with Cas9-RNPs. *Sci. Rep.* **2019**, *9*, 4811. [[CrossRef](#)] [[PubMed](#)]
13. Ferrando, R.E.; Newton, K.; Chu, F.; Webster, J.D.; French, D.M. Immunohistochemical detection of FLAG-tagged endogenous proteins in knock-in mice. *J. Histochem. Cytochem.* **2015**, *63*, 244–255. [[CrossRef](#)] [[PubMed](#)]
14. Zhang, X.; Liang, P.; Ding, C.; Zhang, Z.; Zhou, J.; Xie, X.; Huang, R.; Sun, Y.; Sun, H.; Zhang, J.; et al. Efficient Production of Gene-Modified Mice using Staphylococcus aureus Cas9. *Sci. Rep.* **2016**, *6*, 32565. [[CrossRef](#)] [[PubMed](#)]
15. Imainatsu, K.; Fujii, W.; Hiramatsu, R.; Miura, K.; Kurohmaru, M.; Kanai, Y. CRISPR/Cas9-mediated knock-in of the murine Y chromosomal Sry gene. *J. Reprod. Dev.* **2018**, *64*, 283–287. [[CrossRef](#)] [[PubMed](#)]
16. Vyas, P.; Wood, M.B.; Zhang, Y.; Goldring, A.C.; Chakir, F.Z.; Fuchs, P.A.; Hiel, H. Characterization of HA-tagged  $\alpha$ 9 and  $\alpha$ 10 nAChRs in the mouse cochlea. *Sci. Rep.* **2020**, *10*, 21814. [[CrossRef](#)]
17. Nieto-Rostro, M.; Ramgoolam, K.; Pratt, W.S.; Kulik, A.; Dolphin, A.C. Ablation of  $\alpha$ 2delta-1 inhibits cell-surface trafficking of endogenous N-type calcium channels in the pain pathway in vivo. *Proc. Natl. Acad. Sci. USA* **2018**, *115*, E12043–E12052. [[CrossRef](#)] [[PubMed](#)]

18. Nakano, H.; Kawai, S.; Ooki, Y.; Chiba, T.; Ishii, C.; Nozawa, T.; Utsuki, H.; Umemura, M.; Takahashi, S.; Takahashi, Y. Functional validation of epitope-tagged ATF5 knock-in mice generated by improved genome editing of oviductal nucleic acid delivery (i-GONAD). *Cell Tissue Res.* **2021**, *385*, 239–249. [[CrossRef](#)] [[PubMed](#)]
19. Paul, W.; Frankland, C.O.B.; Ohno, M.; Kirkwood, A.; Silva, A.J.  $\alpha$ -CaMKII-dependent plasticity in the cortex is required for permanent memory. *Nature* **2001**, *411*, 310–313.
20. Akita, T.; Aoto, K.; Kato, M.; Shiina, M.; Mutoh, H.; Nakashima, M.; Kuki, I.; Okazaki, S.; Magara, S.; Shiihara, T.; et al. De novo variants in CAMK2A and CAMK2B cause neurodevelopmental disorders. *Ann. Clin. Transl. Neurol.* **2018**, *5*, 280–296. [[CrossRef](#)]
21. Mutoh, H.; Aoto, K.; Miyazaki, T.; Fukuda, A.; Saitsu, H. Elucidation of pathological mechanism caused by human disease mutation in CaMKII $\beta$ . *J. NeuroSci. Res.* **2022**, *100*, 880–896. [[CrossRef](#)]
22. Chao, L.H.; Stratton, M.M.; Lee, I.H.; Rosenberg, O.S.; Levitz, J.; Mandell, D.J.; Kortemme, T.; Groves, J.T.; Schulman, H.; Kuriyan, J. A mechanism for tunable autoinhibition in the structure of a human Ca<sup>2+</sup>/calmodulin-dependent kinase II holoenzyme. *Cell* **2011**, *146*, 732–745. [[CrossRef](#)]
23. Mikuni, T.; Nishiyama, J.; Sun, Y.; Kamasawa, N.; Yasuda, R. High-Throughput, High-Resolution Mapping of Protein Localization in Mammalian Brain by In Vivo Genome Editing. *Cell* **2016**, *165*, 1803–1817. [[CrossRef](#)]
24. Tunyasuvunakool, K.; Adler, J.; Wu, Z.; Green, T.; Zielinski, M.; Zidek, A.; Bridgland, A.; Cowie, A.; Meyer, C.; Laydon, A.; et al. Highly accurate protein structure prediction for the human proteome. *Nature* **2021**, *596*, 590–596. [[CrossRef](#)]
25. Mirdita, M.; Schütze, K.; Moriawaki, Y.; Heo, L.; Ovchinnikov, S.; Steinegger, M. ColabFold: Making protein folding accessible to all. *Nat. Methods* **2022**, *19*, 679–682. [[CrossRef](#)]
26. Fritzwanker, S.; Mouldous, L.; Mollereau, C.; Froment, C.; Burlet-Schiltz, O.; Effah, F.; Bailey, A.; Spetea, M.; Reinscheid, R.K.; Schulz, S.; et al. HA-MOP knockin mice express the canonical micro-opioid receptor but lack detectable splice variants. *Commun. Biol.* **2021**, *4*, 1070. [[CrossRef](#)]
27. Chamberlain, C.E.; Jeong, J.; Guo, C.; Allen, B.L.; McMahon, A.P. Notochord-derived Shh concentrates in close association with the apically positioned basal body in neural target cells and forms a dynamic gradient during neural patterning. *Development* **2008**, *135*, 1097–1106. [[CrossRef](#)]
28. Sasaki, F.; Okuno, T.; Saeki, K.; Min, L.; Onohara, N.; Kato, H.; Shimizu, T.; Yokomizo, T. A high-affinity monoclonal antibody against the FLAG tag useful for G-protein-coupled receptor study. *Anal. Biochem.* **2012**, *425*, 157–165. [[CrossRef](#)]
29. Yamagata, Y.; Kobayashi, S.; Umeda, T.; Inoue, A.; Sakagami, H.; Fukaya, M.; Watanabe, M.; Hatanaka, N.; Totsuka, M.; Yagi, T.; et al. Kinase-dead knock-in mouse reveals an essential role of kinase activity of Ca<sup>2+</sup>/calmodulin-dependent protein kinase II $\alpha$  in dendritic spine enlargement, long-term potentiation, and learning. *J. NeuroSci.* **2009**, *29*, 7607–7618. [[CrossRef](#)]
30. Carme Solà, J.M.T.; Serratos, J. Decreased Expression of Calmodulin Kinase II and Calcineurin Messenger RNAs in the Mouse Hippocampus After Kainic Acid-Induced Seizures. *J. Neurochem.* **1998**, *70*, 1600–1608. [[CrossRef](#)] [[PubMed](#)]
31. van Breugel, M.; Rosa, E.S.I.; Andreeva, A. Structural validation and assessment of AlphaFold2 predictions for centrosomal and centriolar proteins and their complexes. *Commun. Biol.* **2022**, *5*, 312. [[CrossRef](#)]
32. Alerasool, N.; Leng, H.; Lin, Z.Y.; Gingras, A.C.; Taipale, M. Identification and functional characterization of transcriptional activators in human cells. *Mol. Cell* **2022**, *82*, 677–695. [[CrossRef](#)]
33. Schmidt, A.; Röner, S.; Mai, K.; Klinkhammer, H.; Kircher, M.; Ludwig, K.U. Predicting the pathogenicity of missense variants using features derived from AlphaFold2. *bioRxiv* **2022**. [[CrossRef](#)]
34. Diwan, G.D.; Gonzalez-Sanchez, J.C.; Apic, G.; Russell, R.B. Next Generation Protein Structure Predictions and Genetic Variant Interpretation. *J. Mol. Biol.* **2021**, *433*, 167180. [[CrossRef](#)]
35. McBride, J.M.; Plev, K.; Reinharz, V.; Grzybowski, B.A.; Tlusty, T. AlphaFold2 can predict structural and phenotypic effects of single mutations. *arXiv* **2022**, arXiv:2204.06860.
36. Li, K.; Wang, G.; Andersen, T.; Zhou, P.; Pu, W.T. Optimization of genome engineering approaches with the CRISPR/Cas9 system. *PLoS ONE* **2014**, *9*, e105779. [[CrossRef](#)] [[PubMed](#)]
37. Han, J.P.; Chang, Y.J.; Song, D.W.; Choi, B.S.; Koo, O.J.; Yi, S.Y.; Park, T.S.; Yeom, S.C. High Homology-Directed Repair Using Mitosis Phase and Nucleus Localizing Signal. *Int. J. Mol. Sci.* **2020**, *21*, 3747. [[CrossRef](#)]
38. Kurihara, T.; Kouyama-Suzuki, E.; Satoga, M.; Li, X.; Badawi, M.; Baig, D.N.; Yanagawa, T.; Uemura, T.; Mori, T.; Tabuchi, K. DNA repair protein RAD51 enhances the CRISPR/Cas9-mediated knock-in efficiency in brain neurons. *Biochem. Biophys. Res. Commun.* **2020**, *524*, 621–628. [[CrossRef](#)]
39. Sato, M.; Miyagasako, R.; Takabayashi, S.; Ohtsuka, M.; Hatada, I.; Horii, T. Sequential i-GONAD: An Improved In Vivo Technique for CRISPR/Cas9-Based Genetic Manipulations in Mice. *Cells* **2020**, *9*, 546. [[CrossRef](#)] [[PubMed](#)]
40. Mizuno, N.; Mizutani, E.; Sato, H.; Kasai, M.; Ogawa, A.; Suchy, F.; Yamaguchi, T.; Nakauchi, H. Intra-embryo Gene Cassette Knockin by CRISPR/Cas9-Mediated Genome Editing with Adeno-Associated Viral Vector. *iScience* **2018**, *9*, 286–297. [[CrossRef](#)] [[PubMed](#)]
41. Chen, S.; Sun, S.; Moonen, D.; Lee, C.; Lee, A.Y.; Schaffer, D.V.; He, L. CRISPR-READI: Efficient Generation of Knockin Mice by CRISPR RNP Electroporation and AAV Donor Infection. *Cell Rep.* **2019**, *27*, 3780–3789.e4. [[CrossRef](#)]